Earth Syst. Sci. Data, 15, 171–187, 2023
https://doi.org/10.5194/essd-15-171-2023

Open Access Earth System Science Data

Large freshwater-influx-induced salinity gradient and diagenetic changes in the northern Indian Ocean dominate the stable oxygen isotopic variation in *Globigerinoides ruber*

Rajeev Saraswat[1], Thejasino Suokhrie[1], Dinesh K. Naik[2], Dharmendra P. Singh[3], Syed M. Saalim[4], Mohd Salman[1,5], Gavendra Kumar[1,5], Sudhira R. Bhadra[1], Mahyar Mohtadi[6], Sujata R. Kurtarkar[1], and Abhayanand S. Maurya[3]

[1]Micropaleontology Laboratory, Geological Oceanography Division, National Institute of Oceanography, Goa, India
[2]Department of Geology, Banaras Hindu University, Varanasi, Uttar Pradesh, India
[3]Department of Earth Sciences, Indian Institute of Technology–Roorkee (IIT–Roorkee), Roorkee, Uttarakhand, India
[4]Antarctic Science Division, National Center for Polar and Ocean Research, Goa, India
[5]School of Earth, Ocean and Atmospheric Sciences, Goa University, Goa, India
[6]Center for Marine Environmental Sciences (MARUM), University of Bremen, Bremen, Germany

Correspondence: Rajeev Saraswat (rsaraswat@nio.org)

Received: 29 March 2022 – Discussion started: 6 July 2022
Revised: 22 November 2022 – Accepted: 23 November 2022 – Published: 10 January 2023

Abstract. The application of stable oxygen isotopic ratio of surface-dwelling planktic foraminifera *Globigerinoides ruber* (white variety; $\delta^{18}O_{ruber}$) to reconstruct past hydrological changes requires a precise understanding of the effect of ambient parameters on $\delta^{18}O_{ruber}$. The northern Indian Ocean, with its huge freshwater influx and being a part of the Indo-Pacific Warm Pool, provides a unique setting to understand the effect of both the freshwater-influx-induced salinity and temperature on $\delta^{18}O_{ruber}$. Here, we use a total of 400 surface samples (252 from this work and 148 from previous studies), covering the entire salinity end-member region, to assess the effect of freshwater-influx-induced seawater salinity and temperature on $\delta^{18}O_{ruber}$ in the northern Indian Ocean. The analysed surface $\delta^{18}O_{ruber}$ mimics the expected $\delta^{18}O$ calcite estimated from the modern seawater parameters (temperature, salinity, and seawater $\delta^{18}O$) very well. We report a large diagenetic overprinting of $\delta^{18}O_{ruber}$ in the surface sediments, with an increase of 0.18 ‰ per kilometre increase in water depth. The freshwater-influx-induced salinity exerts the major control on $\delta^{18}O_{ruber}$ ($R^2 = 0.63$) in the northern Indian Ocean, with an increase of 0.29 ‰ per unit increase in salinity. The relationship between temperature- and salinity-corrected $\delta^{18}O_{ruber}$ ($\delta^{18}O_{ruber} - \delta^{18}O_{sw}$) in the northern Indian Ocean [$T = -0.59 \cdot (\delta^{18}O_{ruber} - \delta^{18}O_{sw}) + 26.40$] is different than reported previously, based on the global compilation of plankton tow $\delta^{18}O_{ruber}$ data. The revised equations will help create a better palaeoclimatic reconstruction from the northern Indian Ocean by using the stable oxygen isotopic ratio. The entire data set (newly generated and previously published) used in this work is available both as a Supplement to this article and at PANGAEA (https://doi.org/10.1594/PANGAEA.945401; Saraswat et al., 2022).

Published by Copernicus Publications.

1 Introduction

The stable oxygen isotopic ratio ($\delta^{18}O$) of biogenic carbonates is one of the most extensively used marine palaeoclimatic proxies (Mulitza et al., 1997; Lea, 2014; Metcalfe et al., 2019; Saraswat et al., 2019). Even though it was initially suggested that the oxygen isotopic fractionation in biogenic carbonates is largely driven by temperature (Urey, 1947), subsequent work revealed that, besides temperature, the salinity and carbonate ion concentration of ambient seawater also affects the biogenic carbonate $\delta^{18}O$ (Vergnaud-Grazzini, 1976; Spero et al., 1997; Bemis et al., 1998; Spero et al., 1997; Bijma et al., 1999; Mulitza et al., 2003). On longer timescales, the global ice volume contribution to the glacial–interglacial shift in marine biogenic carbonate $\delta^{18}O$ is the largest ($\sim 1.0‰$–$1.2‰$) at a majority of the locations (Shackleton, 1987, 2000; Lambeck et al., 2014). The ice volume changes have induced well-defined globally similar shifts in biogenic carbonate $\delta^{18}O$ during the last several million years. Therefore, the regional evaporation–precipitation, runoff, and temperature changes are reconstructed from the global ice-volume-corrected biogenic carbonate $\delta^{18}O$ (Wang et al., 1995; Kallel et al., 1997; Schmidt et al., 2004; Saraswat et al., 2012, 2013; Kessarkar et al., 2013).

The $\delta^{18}O$ of surface-dwelling planktic foraminifera *Globigerinoides ruber* ($\delta^{18}O_{ruber}$) is often used to reconstruct past surface seawater conditions (Pearson, 2012; Saraswat et al., 2012, 2013; Mahesh and Banakar, 2014). Therefore, continuous efforts are made to understand the factors affecting $\delta^{18}O_{ruber}$ (Vergnaud-Grazzini, 1976; Mulitza et al., 1997, 1998, 2003; Waelbroeck et al., 2005; Mohtadi et al., 2011; Horikawa et al., 2015; Hollstein et al., 2017; Sánchez et al., 2022). The depth habitat of *G. ruber* in the tropical Atlantic Ocean has been inferred from its stable oxygen isotopic ratio (Farmer et al., 2007). The change in the stable oxygen isotopic ratio of planktic foraminifera, including *G. ruber*, is suggested as a proxy to reconstruct the upper water column stratification in the tropical Atlantic Ocean, based on the good correlation between $\delta^{18}O$ and the ambient seawater characteristics (Steph et al., 2009). A few studies suggested a difference in the $\delta^{18}O$ of the various morphotypes of *G. ruber* (sensu stricto and sensu lato) and attributed it to their distinct ecology and depth habitat (Löwemark et al., 2005). However, a recent study from the Gulf of Mexico suggested a similar ecology and depth habitat for both the *G. ruber* morphotypes (Thirumalai et al., 2014). The northern Indian Ocean, being influenced by huge freshwater influx and being part of the Indo-Pacific Warm Pool (De Deckker, 2016), provides a unique setting to understand the effect of large salinity and temperature changes on $\delta^{18}O_{ruber}$. Earlier, Duplessy et al. (1981a) measured the $\delta^{18}O$ of the living *G. ruber* specimens collected from the water column and the dead ones recovered from surface sediments of the northern Indian Ocean. A similar study from the Red Sea and adjoining western Arabian Sea suggested that *G. ruber* calcifies its test in isotopic equilibrium with the ambient seawater, thus tracking the interannual subtle change in the salinity and temperature (Kroon and Ganssen, 1989; Ganssen and Kroon, 1991).

The temperature influence on $\delta^{18}O_{ruber}$ is well defined (Shackleton and Vincent, 1978; Multiza et al., 1998, 2003). The effect of freshwater-influx-induced changes in ambient salinity on $\delta^{18}O_{ruber}$ is, however, debated (Dämmer et al., 2020). With the extensive use of $\delta^{18}O_{ruber}$ to reconstruct regional evaporation–precipitation changes, especially from the monsoon-dominated tropical oceans, it is imperative to understand the precise influence of ambient salinity on $\delta^{18}O_{ruber}$. The ambient seawater pH, carbonate ion concentration (Bijma et al., 1999), and presence/absence of symbionts (Jørgensen et al., 1985) also affect the isotopic composition of *G. ruber*. However, a limited glacial–interglacial variability in these parameters is masked by the dominance of temperature and freshwater-influx-induced salinity changes in the oxygen isotopic ratio of *G. ruber*. Additionally, the diagenetic changes, especially dissolution, also substantially alter the original isotopic composition of the foraminifera shells (Berger and Killingley, 1977; Wu and Berger, 1989; Lohmann, 1995; McCorkle et al., 1997; Wycech et al., 2018). The dissolution preferentially removes the lighter-oxygen sections of the shells, thus increasing the whole shell $\delta^{18}O_{ruber}$ (Berger and Gardner, 1975; Lohmann, 1995; Weinkauf et al., 2020). The studies based on the comparison of ambient parameters with the isotopic composition of living specimens collected in plankton tows may neither address the complete range of the changes in the isotopic signatures during the sinking of the tests from the surface waters post-death nor its subsequent deposition in the sediments at the bottom of the sea. As the fossil shells are the sole basis for finding out the isotopic ratio of the ambient seawater in the past, the effect of diagenetic changes including the dissolution on foraminifer's oxygen isotopic ratio has to be properly evaluated. Here, we assess the influence of freshwater-influx-induced strong salinity gradient, ambient temperature, depth-induced dissolution, and other associated parameters on the stable oxygen isotopic ratio of the surface-dwelling planktic foraminifera *G. ruber* (white variety) in the surface sediments of the northern Indian Ocean.

2 Ecology of *Globigerinoides ruber* (white)

Globigerinoides ruber is a spinose planktic foraminifera inhabiting the mixed layer waters, throughout the year, in the tropical–subtropical regions (Guptha et al., 1997; Kemle-von-Mücke and Hemleben, 1999; Stainbank et al., 2019). It is one of the dominant planktic foraminifera in the northern Indian Ocean (Bé and Hutson, 1977; Bhadra and Saraswat, 2021), with its relative abundance being as high as $\sim 60\,\%$ (Fraile et al., 2008). Its test is medium to low trochospiral, and it hosts algal symbionts (Hemleben et al., 1989). *Globigerinoides ruber* prefers to feed upon phytoplankton

(Hemleben et al., 1989) and is dominant in oligotrophic warmer water, with the optimal temperature being 23.5 °C (Fraile et al., 2008). However, it is amongst a few planktic foraminifera species that can tolerate a wide range of salinity (22–49 psu) and temperature (14–31 °C; Hemleben et al., 1989; Guptha et al., 1997). Two varieties of *G. ruber*, namely the white and pink, are common in the world oceans. However, the pink variety of *G. ruber* became extinct in the Indian and Pacific oceans at ∼ 120 kyr during the Marine Isotopic Stage 5e (Thompson et al., 1979).

3 Northern Indian Ocean

The Indian Ocean, with its northern boundary in the tropics, includes two hydrographically contrasting basins, namely the Arabian Sea and Bay of Bengal (BoB; Fig. 1). The excess of evaporation over precipitation generates a high-salinity water mass that spreads throughout the surface of the northern Arabian Sea, with its core as deep as ∼ 100 m (Shetye et al., 1994; Prasanna Kumar and Prasad, 1999; Joseph and Freeland, 2005). Other high-salinity water masses from both the Persian Gulf and Red Sea enter the northern Arabian Sea at deeper depths between 200–400 and 500–800 m, respectively (Rochford, 1964). A strong upwelling along the western boundary of the Arabian Sea during the summer monsoon season brings cold, nutrient-rich subsurface waters to the surface (Chatterjee et al., 2019). The weak upwelling during the same season is also reported in the southeastern Arabian Sea (Smitha et al., 2014).

The surface water is relatively fresher in the BoB, as the majority of the rivers from the Indian subcontinent drain here, with the total annual continental runoff amounting to 2950 km^3 (Sengupta et al., 2006). Additionally, the total annual precipitation over the BoB is 4700 km^3, and the evaporation is 3600 km^3 (Sengupta et al., 2006). The high-salinity water in the Arabian Sea is transported into the BoB, and the fresher BoB water mixes with the high-salinity water in the Arabian Sea by the seasonally reversing coastal currents (Shankar et al., 2002). The upwelling during summer is restricted to only the northwestern part of the BoB (Shetye et al., 1991). The upwelling combined with the convective mixing during the winter season in the northeastern Arabian Sea (Madhupratap et al., 1996), in addition to eddies in the BoB (Prasanna Kumar et al., 2004; Sarma et al., 2020), result in very high primary productivity in both basins (Qasim, 1977; Prasanna Kumar et al., 2009). The high primary productivity and freshwater capping induce strong stratification and restricted circulation that create oxygen-deficient zones (ODZs) at the intermediate depth in both the Arabian Sea (Rixen et al., 2020; Naqvi, 2021) and BoB (Bristow et al., 2017; Sridevi and Sarma, 2020). The Arabian Sea ODZ, however, is comparatively thicker and more intense, leading to denitrification (Naqvi et al., 2006), which has not yet been reported from the BoB (Bristow et al., 2017).

The equatorial Indian Ocean forms a part of the Indo-Pacific Warm Pool, with the sea surface temperature at > 28 °C throughout the year (Vinayachandran and Shetye, 1991; De Deckker, 2016). The marginal regions of the BoB are comparatively warmer due to the freshwater influx from the rivers. The riverine influx shoals the mixed layer and thickens the barrier layer, a buoyant layer separating the thermocline from the pycnocline, in the BoB (Howden and Murtugudde, 2001). The riverine influx flows as a low-salinity tongue all along the eastern margin of India (Chaitanya et al., 2014). The annual average sea surface salinity (SSS) is < 34 psu throughout the BoB, increasing from the head bay towards the south. In contrast to that, SSS remains at > 35 psu almost throughout the year in the Arabian Sea (Rao and Sivakumar, 2003). The excess of evaporation over precipitation, due to the dry northeasterly winds, leads to the highest salinity in the northern BoB during the winter (Rao and Sivakumar, 2003).

4 Materials and methodology

The surface sediments were collected all along the path of the seasonal coastal currents in the northern Indian Ocean (Fig. 2; Table S1 in the Supplement). The samples from the Ayeyarwady delta shelf in the northeastern BoB were collected during the India–Myanmar Joint Oceanographic Studies on board the ocean research vessel (R/V) *Sagar Kanya* (SK175). A total of 110 surface sediment samples were collected from the water depths, ranging from 10 to 1080 m, on the Ayeyarwady delta shelf (Ramaswamy et al., 2008). The multicore samples were also collected at regular intervals in transects running perpendicular to the coast from the western BoB during cruise SK308, on board R/V *Sindhu Sadhana* (cruise SSD067), and on board R/V *Sindhu Sankalp* (cruise SSK35). A total of 84 surface samples (including 71 multicore samples and 13 grab samples from sandy sediments) were collected from the inner shelf to outer slope region of the eastern margin of India during cruise SK308 (Suokhrie et al., 2021; Saalim et al., 2022). These samples from the western BoB represent the lowest-salinity region in the northern Indian Ocean (Panchang and Nigam, 2012). The multicore samples collected between 25 and 2980 m in the Gulf of Mannar and the region to the west of it (43 samples on board R/V *Sindhu Sadhana* during cruise SSD004) represent the zone of cross-basin exchange of seawater between the BoB and the Arabian Sea (Singh et al., 2021). The spade core samples collected from the southeastern Arabian Sea (R/V *Sagar Kanya* during cruise SK117 and SK237) are located close to the distal end of the low-salinity BoB water intruding into the Arabian Sea. The multicore samples (13 in number) collected during SSD055 cruise, from the northeastern Arabian Sea, represent the warm saline conditions. We also collected spade core surface samples from the Andaman Sea, on board R/V *Sindhu Sankalp* (cruise SSK98). A total of 252 sam-

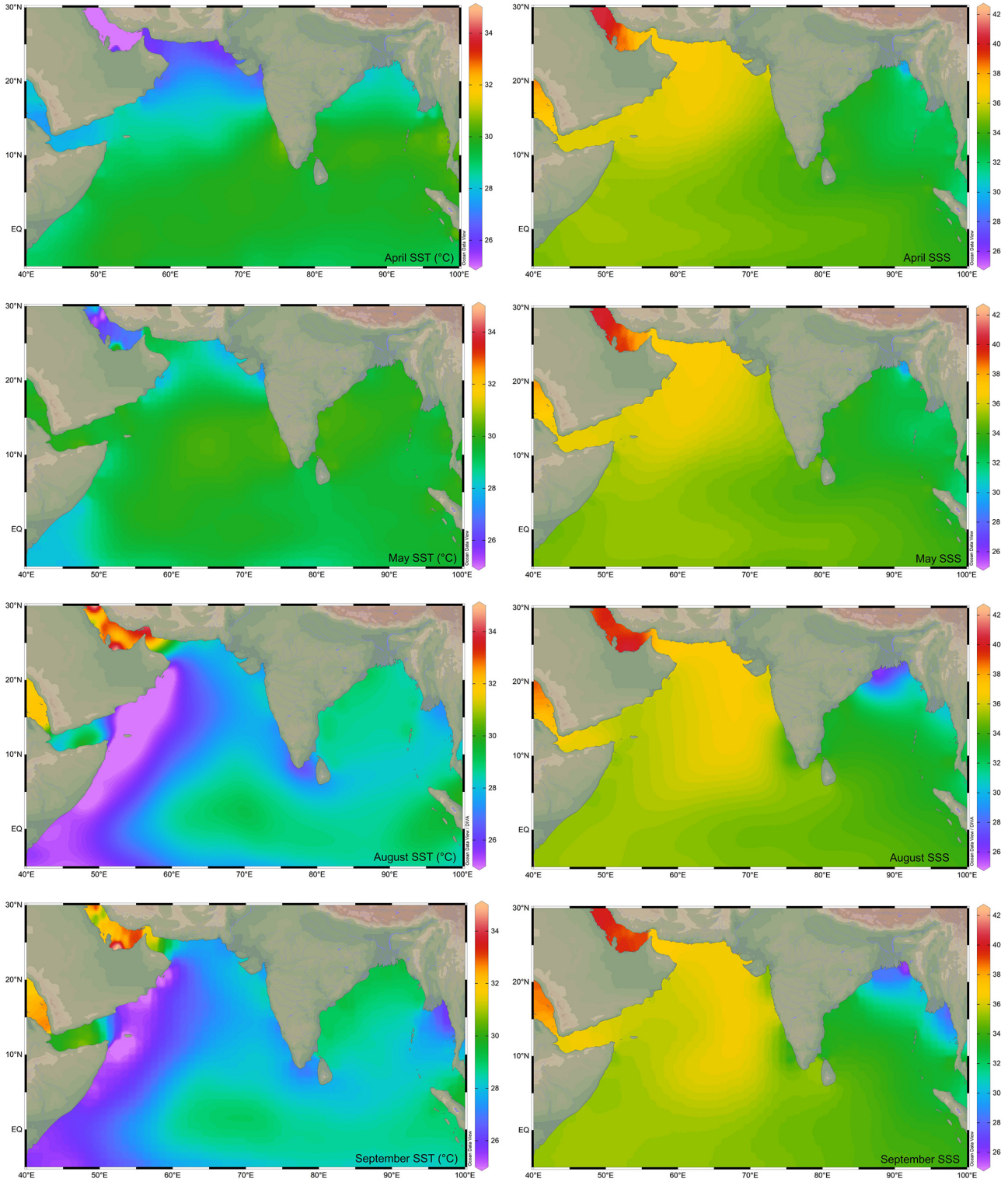

Figure 1. The sea surface temperature (SST; °C; Locarnini et al., 2018) and sea surface salinity (SSS; psu; Zweng et al., 2018) in the northern Indian Ocean during the monsoon (August–September) and non-monsoon (April–May) months. The major rivers draining into the northern Indian Ocean are marked by thin blue lines. The map has been prepared by using Ocean Data View software (Schlitzer, 2018).

ples had sufficient *G. ruber* for an isotopic analysis (Table 1). The new data were augmented with 148 previously published core-top studies (e.g. Sirocko, 1989; Prell and Curry, 1981; Duplessy et al., 1981a; Duplessy, 1982) mainly compiled by Waelbroeck et al. (2005). Therefore, a total of 400 surface sample data points were used for this study.

The surface sediment samples (0–1 cm) were processed following the standard procedure (Suokhrie et al., 2022). The freeze-dried sediments were weighed and wet-sieved by using a 63 µm sieve. Part of the coarse fraction (> 63 µm) was dry-sieved by using 250 µm and 355 µm sieves. For $\delta^{18}O$ analysis, 10–15 well-preserved shells of the *G. ruber* white variety were picked from 250 to 355 µm size range. We picked *G. ruber* sensu stricto wherever sufficient specimens were available. Unfortunately, several samples yielded a very small carbonate fraction. In such samples, we picked a mixed population of *G. ruber* to have sufficient specimens for isotopic analysis. The $\delta^{18}O_{ruber}$ was measured by using Thermo Scientific MAT 253 isotope ratio mass spectrometer coupled with a Kiel IV automated carbonate preparation device. The samples were analysed at the Alfred Wegener Institute for Polar and Marine Research, Bremerhaven (MARUM, University of Bremen, Bremen, Germany) and the Stable Isotope Laboratory (SIL) at Indian Institute of Technology, Roorkee, India. Reference material from the National Bureau of Standards (NBS 18/19) limestone was used as the calibration material, and a secondary in-house standard was run after every five samples to detect and correct the drift. The precision of oxygen isotope measurements was better than 0.08 ‰. The $\delta^{18}O_{ruber}$ data generated on the newly collected surface sediments was augmented with the published core-top $\delta^{18}O$ measurements in the northern Indian Ocean. A total of 400 surface sediment data points (252 from this work and 148 from the previous studies) were used to understand the factors affecting $\delta^{18}O_{ruber}$ in the northern Indian Ocean (Table S1 in the Supplement). The annual average sea surface temperature and salinity of the top 30 m of the water column at the respective sample locations was downloaded from the World Ocean Atlas (Boyer et al., 2013). The salinity and temperature at the core location was extrapolated from the nearby grid points using the live-access server at the National Institute of Oceanography, Goa, India.

The analysed $\delta^{18}O_{ruber}$ data were compared with the expected $\delta^{18}O$ calcite to ascertain whether the *G. ruber* properly represents the ambient conditions. For the expected $\delta^{18}O$ calcite, the $\delta^{18}O_{sw}$ was calculated from the ambient salinity by using a compilation of the regional seawater salinity and its stable oxygen isotopic ($\delta^{18}O_{sw}$) ratio data for the entire northern Indian Ocean (5° S to 30° N). The seawater salinity and corresponding $\delta^{18}O_{sw}$ data were downloaded from Schmidt et al. (1999; version 1.22) and augmented with other regional data sets (Delaygue et al., 2001; Singh et al., 2010; Achyuthan et al., 2013).

5 Results

The oxygen isotopic ratio of *G. ruber* varied from a minimum of −3.82 ‰ to the maximum of −1.09 ‰ in the surface sediments of the northern Indian Ocean (Fig. 3). The most depleted $\delta^{18}O_{ruber}$ was in the eastern BoB, and the most enriched values were in the western Arabian Sea.

The east–west gradient in $\delta^{18}O_{ruber}$ was also evident in its significant correlation ($R^2 = 0.5$, $n = 400$) with the longitude (Fig. 4a). However, $\delta^{18}O_{ruber}$ did not have any systematic latitudinal variation (Fig. 4b).

A significant correlation ($R^2 = 0.14$; $n = 400$) was observed between the water depth and $\delta^{18}O_{ruber}$ (Fig. 5). $\delta^{18}O_{ruber}$ increased with increasing depth. The increase was gradual, without any abrupt change.

The uncorrected $\delta^{18}O_{ruber}$ was significantly correlated ($R^2 = 0.63$; $n = 400$) with the ambient salinity (Fig. 6a). However, the relationship between uncorrected $\delta^{18}O_{ruber}$ and ambient temperature was not as robust ($R^2 = 0.18$; $n = 400$; Fig. 6b). A large scatter (∼ −3.8 ‰ to −1.4 ‰) was observed in the $\delta^{18}O_{ruber}$ of the samples collected from a narrow range of ambient temperature (28–29 °C; Fig. 6b).

As the northern Indian Ocean includes two contrasting basins, the $\delta^{18}O_{ruber}$–salinity relationship was explored for both the Arabian Sea and the BoB. A significant $\delta^{18}O_{ruber}$–salinity relationship was observed for both the Arabian Sea ($R^2 = 0.28$; $n = 205$) and BoB ($R^2 = 0.14$; $n = 195$; Fig. 7). We report a different $\delta^{18}O_{ruber}$–salinity relationship in these two basins. $\delta^{18}O_{ruber}$ increased with increasing salinity in both the BoB and the Arabian Sea.

The data set to derive the regional salinity–$\delta^{18}O_{sw}$ relationship comprised of a total of 750 stations, with salinity varying from 20.92 to 40.91 psu (Schmidt et al., 1999). The data set also covered a large range of $\delta^{18}O_{sw}$, varying from a minimum of −2.45 ‰ to the maximum of 2.02 ‰ (Figs. 8 and 9). The measured $\delta^{18}O_{ruber}$ was strongly correlated ($R^2 = 0.56$; $n = 400$) with the expected $\delta^{18}O_{calcite}$, as estimated by using the salinity–$\delta^{18}O_{sw}$ relationship and the ambient temperature. However, the relationship between seawater temperature and $\delta^{18}O_{ruber}$–$\delta^{18}O_{sw}$ was not very robust. It should, however, be noted here that the stratigraphic information is not provided for most of the core tops. The core-top sediments can represent older time slices when the sedimentation rates are low or when older sediments are exposed due to erosional processes. This does not matter so much if the Holocene is present and stable. However, in the Indian Ocean, large Holocene $\delta^{18}O$ variations are expected due to variations in monsoon precipitation. Therefore, the uncertain age of the core tops can affect the results stated above.

Table 1. Details of the timing, region, and the number of surface sediment samples collected in each expedition used in this study (SK is *Sagar Kanya*, SSD is *Sindhu Sadhana*, and SSK is *Sindhu Sankalp*).

Serial no.	Cruise	Month/year	Area	Total samples
1.	SK117	September–October 1996	Eastern Arabian Sea	27
2.	SK175	April–May 2002	Northeastern Bay of Bengal	45
3.	SK237	August 2007	Southeastern Arabian Sea	26
4.	SK308	January 2014	Northwestern Bay of Bengal	29
5.	SSD004	October–November 2014	Gulf of Mannar, Lakshadweep Sea	41
6.	SSD055	August 2018	Northeastern Arabian Sea	11
7.	SSD067	November–December 2019	Southwestern Bay of Bengal, Lakshadweep Sea, eastern Arabian Sea	45
8.	SSK035	May–June 2012	Western Bay of Bengal	13
9.	SSK098	January–February 2017	Andaman Sea	15

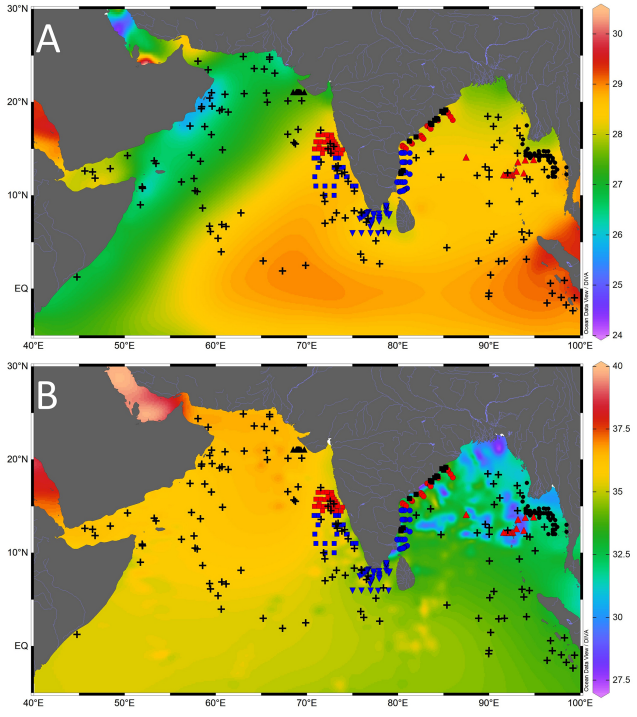

Figure 2. Location of the core-top samples analysed in this study (black-filled triangle is cruise SSD055, red-filled square is cruise SK117, blue-filled square is cruise SK237, blue-filled inverted triangle is cruise SSD004, blue-filled circle is cruise SSD067, red-filled circle is cruise SK308, black-filled square is cruise SSK035, red-filled triangle is cruise SSK098, and black-filled circle is cruise SK175), and the previously published core-top values (black plus sign) compiled from the northern Indian Ocean. The background contours are temperature (°C) **(a)** and salinity (psu) **(b)**, with the scale on the right. Major rivers draining into the northern Indian Ocean are marked by thin blue lines. The map was prepared by using Ocean Data View software (Schlitzer, 2018).

6 Discussion

6.1 Expected versus analysed $\delta^{18}O$

The seawater $\delta^{18}O$ data are required to estimate the expected $\delta^{18}O$ carbonate. The seawater $\delta^{18}O$, however, was not measured. Therefore, the salinity–$\delta^{18}O_{sw}$ relationship established from the previous regional seawater isotope and salinity measurements was used (Fig. 8). The salinity–$\delta^{18}O_{sw}$ relationship varies seasonally and from region to region (Singh et al., 2010; Achyuthan et al., 2013; Tiwari et al., 2013). Therefore, it was difficult to choose the appropriate salinity–$\delta^{18}O_{sw}$ relationship. Initially, all the data points were clubbed to establish the salinity–$\delta^{18}O_{sw}$ relationship. By comparing the measured $\delta^{18}O_{sw}$ with the ambient salinity, we established the following relationship for the entire northern Indian Ocean (north of 5° S latitude; $R^2 = 0.57$; $n = 750$; Fig. 9):

$$\delta^{18}O_{sw} = 0.16 \cdot \text{salinity} - 4.94$$
Northern Indian Ocean ($R^2 = 0.57$).

Previously, a large difference in the slope of salinity–$\delta^{18}O_{sw}$ equation has been reported from the Arabian Sea and the BoB (Delaygue et al., 2001; Singh et al., 2010; Achyuthan et al., 2013). Therefore, we also plotted the salinity–$\delta^{18}O_{sw}$ separately for the Arabian Sea and BoB (Fig. 9). The salinity–$\delta^{18}O_{sw}$ relationship for these two basins was represented by the following equations:

$$\delta^{18}O_{sw} = 0.10 \cdot \text{salinity} - 2.84$$
Arabian Sea ($R^2 = 0.31,\ n = 375$)

$$\delta^{18}O_{sw} = 0.13 \cdot \text{salinity} - 4.23$$
Bay of Bengal ($R^2 = 0.31,\ n = 375$).

The continuous flux of *G. ruber* throughout the year (Guptha et al., 1997), and the accumulation of shells in the sediments over a large interval, implies that the salinity–$\delta^{18}O_{sw}$ relationship based on data representing all seasons will provide a better estimate of the average $\delta^{18}O_{ruber}$, as recovered

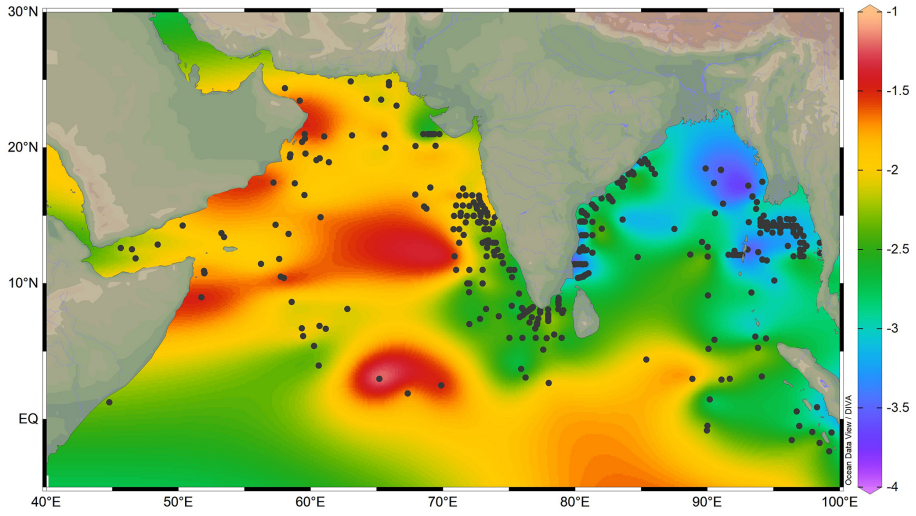

Figure 3. The variation in *Globigerinoides ruber* δ^{18}O (‰) in the surface sediments of the northern Indian Ocean. The stations are marked by a black-filled circle. The lowest $\delta^{18}O_{ruber}$ is in the riverine-influx-influenced northern Bay of Bengal, and the highest is in the evaporation-dominated central and western Arabian Sea. The major rivers are marked with thin blue lines. The map was prepared by using Ocean Data View software (Schlitzer, 2018).

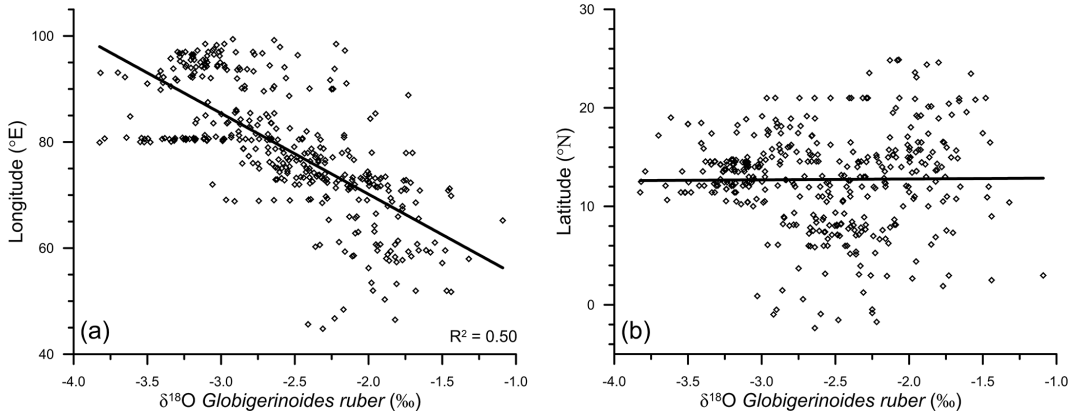

Figure 4. The variation in *Globigerinoides ruber* δ^{18}O (‰), with the corresponding longitude **(a)** and latitude **(b)**, in the surface sediments of the northern Indian Ocean. The correlation between $\delta^{18}O_{\mathbf{ruber}}$ and the latitude of the sample is insignificant.

from the sediments (Vergnaud-Grazzini, 1976). The expected $\delta^{18}O_{sw}$ was calculated by using these equations and the annual average mixed layer salinity at the stations for which $\delta^{18}O_{ruber}$ data were available. The mixed layer was defined as the top 25 m of the water column, following Narvekar and Prasanna Kumar (2014). Although the mixed layer depth varies regionally and during different seasons, the average mixed layer depth was used to compare the calcification conditions. A correction factor of 0.27 ‰ was applied to convert $\delta^{18}O_{sw}$ from Standard Mean Oceanic Water (SMOW) scale to the Pee Dee Belemnite (PDB) scale (Hut, 1987). The expected δ^{18}O calcite was then estimated from the calculated $\delta^{18}O_{sw}$ and the annual average mixed layer temperature by using the equation proposed by Mulitza et al. (2003). We also estimated the expected δ^{18}O calcite by using the high light equation of Bemis et al. (1998), as *G. ruber* δ^{18}O is better described with the high light equation (Thunell et al., 1999). The choice of equation used to estimate the expected δ^{18}O calcite did not make any difference, other than a small offset. The difference between expected δ^{18}O calcite estimated by using palaeotemperature equation of Mulitza et al. (2003) and the high light equation of Bemis et al. (1998) varied from −0.33 ‰ to −0.41 ‰. The expected δ^{18}O calcite estimated by using the Mulitza et al. (2003) palaeotemperature equation provided values close to the measured *G. ruber* δ^{18}O. From the scatterplot (Fig. 10), it was clear that the analysed $\delta^{18}O_{ruber}$ was significantly correlated ($R^2 = 0.56$; $n = 400$) with the expected δ^{18}O calcite, suggesting that *G. ruber* closely represents the ambient conditions in the entire northern Indian Ocean. The expected δ^{18}O calcite esti-

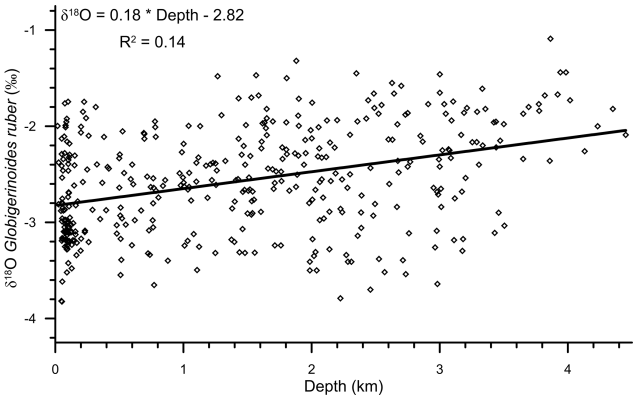

Figure 5. The relationship between water depth and the oxygen isotopic ratio of the mixed-layer-dwelling *Globigerinoides ruber* in the surface sediments of the northern Indian Ocean. The trend line signifies the relative enrichment of $\delta^{18}O_{ruber}$ shells in surface sediments, with increasing water depth. The empirical relationship between the water depth and $\delta^{18}O_{ruber}$ is represented with an equation. The $\delta^{18}O_{ruber}$ is significantly correlated ($R^2 = 0.14$; $n = 400$) with the water depth.

mated by using the separate Arabian Sea and BoB salinity–$\delta^{18}O_{sw}$ equations was also similarly correlated with the analysed $\delta^{18}O_{ruber}$.

The deviation of the expected $\delta^{18}O_{calcite}$ from the observed $\delta^{18}O_{ruber}$ ($\delta^{18}O_{residual}$) can be because of several factors, including the difference in the ambient conditions at the time of the secretion of the primary calcite during the lifetime and the digenetic changes post-death and during the burial. The observed $\delta^{18}O_{ruber}$ was close to the expected $\delta^{18}O_{calcite}$ in the shallower waters, especially the BoB, Andaman Sea, and northeastern Arabian Sea (Fig. 11). The difference was large in the deeper Arabian Sea and the equatorial Indian Ocean. *Globigerinoides ruber* is suggested to inhabit chlorophyll maximum for the easy availability of food (Fairbanks and Wiebe, 1980). In such a scenario, $\delta^{18}O_{ruber}$ is expected to be higher due to lower temperatures and lower light levels at relatively deeper depths (Spero et al., 1997). The depth of chlorophyll maximum is shallower in the marginal marine waters of both the BoB and the Arabian Sea (Sarma and Aswanikumar, 1991; Madhu et al., 2006). If *G. ruber* thrived at chlorophyll maximum depths, then the $\delta^{18}O_{ruber}$ should be enriched in heavier isotope and thus $\delta^{18}O_{residual}$ should be negative. The positive $\delta^{18}O_{residual}$ in the shallower regions, however, suggests that *G. ruber* thrives in the warmer upper parts of the mixed layer. Alternatively, the large influence of the heavier-oxygen-isotope-depleted freshwater $\delta^{18}O$ dominates the chlorophyll maximum influence on the observed $\delta^{18}O_{ruber}$ in the shallower regions of the northern Indian Ocean. The concentration of positive $\delta^{18}O_{residual}$ values close to the riverine influx regions confirms the strong influence of the heavier-oxygen-isotope-depleted freshwater $\delta^{18}O$ in modulating $\delta^{18}O_{ruber}$ in the northern Indian Ocean. The negative $\delta^{18}O_{residual}$ at deeper stations is attributed to a combination of factors including deeper chlorophyll maximum depth habitat of *G. ruber*, the reduced influence of freshwater, a lower sedimentation rate resulting in the mixing of older and younger fauna, and post-depositional digenetic changes.

6.2 Latitudinal and longitudinal variation in $\delta^{18}O_{ruber}$

We report a strong ($R^2 = 0.50$) longitudinal influence on $\delta^{18}O_{ruber}$. A similar relationship with the latitudes is missing. The strong longitudinal signature in $\delta^{18}O_{ruber}$ is attributed to the large salinity gradient. The huge freshwater influx in the BoB reduces the SSS in the eastern Indian Ocean. The lack of major rivers in the western Arabian Sea results in strong low- to high-salinity gradient from east to west. Although the equatorial and nearby regions are a part of the Indo-Pacific Warm Pool, the limited temperature variability is evident in the insignificant latitudinal influence on $\delta^{18}O_{ruber}$.

6.3 Diagenetic alteration

We found a strong diagenetic overprinting of $\delta^{18}O_{ruber}$ in the northern Indian Ocean (Fig. 5). The enrichment of $\delta^{18}O_{ruber}$ with increasing water depth suggests either dissolution, leading to the preferential removal of chambers with a higher fraction of the lighter oxygen isotope (Wycech et al., 2018), or secondary calcification under comparatively colder water (Lohmann, 1995; Schrag et al., 1995). The increase in planktic foraminifera $\delta^{18}O$ with increasing depth is a common diagenetic alteration throughout the world oceans (Bonneau et al., 1980). Interestingly, the extent of the increase in $\delta^{18}O_{ruber}$ with depth in the northern Indian Ocean is much smaller (0.18 ‰ per 1000 m) than that reported for the same species from the Pacific Ocean (0.4 ‰ per 1000 m; Bonneau et al., 1980). However, the increase in $\delta^{18}O_{ruber}$ with depth in the northern Indian Ocean is continuous, unlike the abrupt shift in $\delta^{18}O$ (0.3 ‰–0.4 ‰ between the depths above and below the lysocline) of another surface-dwelling planktic species, namely *Trilobatus sacculifer*, as observed in the western equatorial Pacific (Wu and Berger, 1989). The smaller increase in $\delta^{18}O_{ruber}$ with depth is attributed to the shallower habitat of *G. ruber* as compared to *T. sacculifer*. The chamber formation at different water depths implies increased heterogeneity in the *T. sacculifer* shells, with those formed at warmer surface temperature being more susceptible to dissolution as compared to those formed at deeper depths during the gametogenesis phase (Duplessy et al., 1981b; Wycech et al., 2018). The chambers in *G. ruber* are formed at a similar depth, and therefore, the increase in $\delta^{18}O_{ruber}$ is continuous, while those of *T. sacculifer* are precipitated at different depths, and therefore, the shift in $\delta^{18}O$ occurs after a particular depth. The increase in $\delta^{18}O_{ruber}$ with depth is mainly due to the partial dissolution of the more porous and thinner parts of the shells secreted at warmer temperatures, as such parts are comparatively more susceptible to dissolution (Berger,

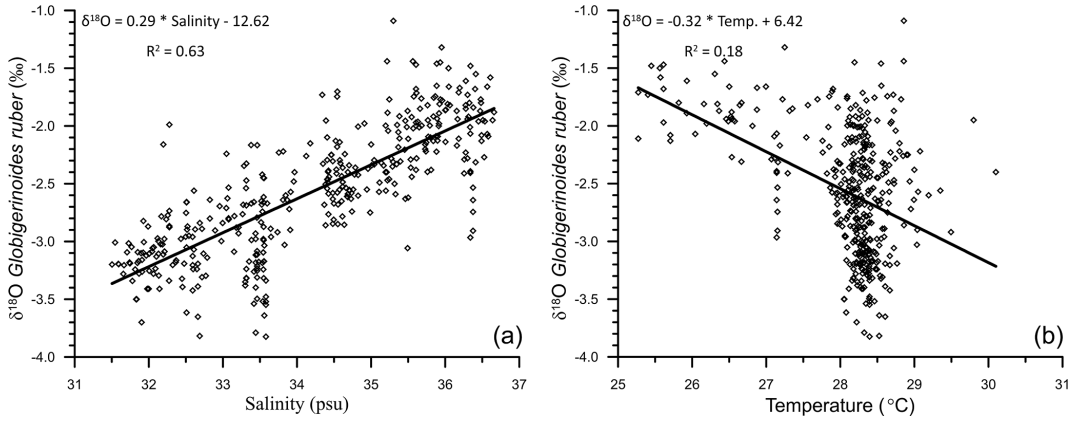

Figure 6. The relationship between the stable oxygen isotopic ratio of the mixed-layer-dwelling *Globigerinoides ruber* and annual average mixed layer salinity **(a)** and temperature **(b)** in the northern Indian Ocean.

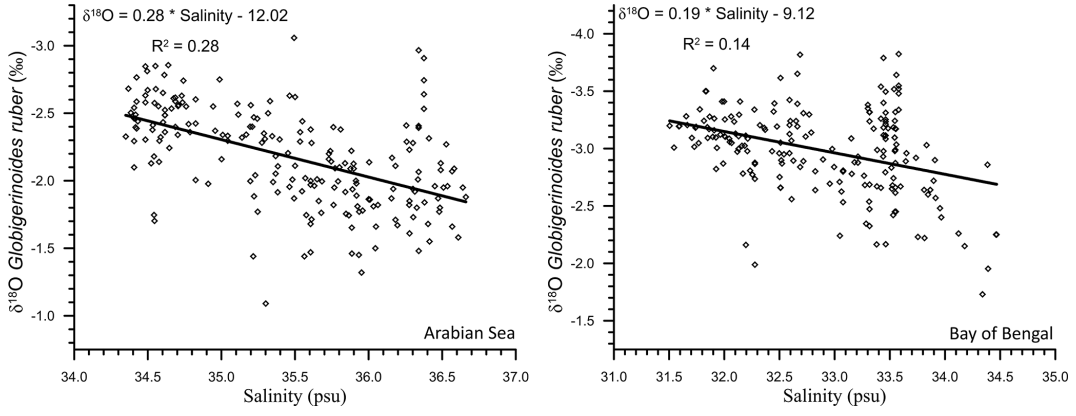

Figure 7. The relationship between the stable oxygen isotopic ratio of the mixed-layer-dwelling *Globigerinoides ruber* and the annual average mixed layer salinity in the Arabian Sea and Bay of Bengal.

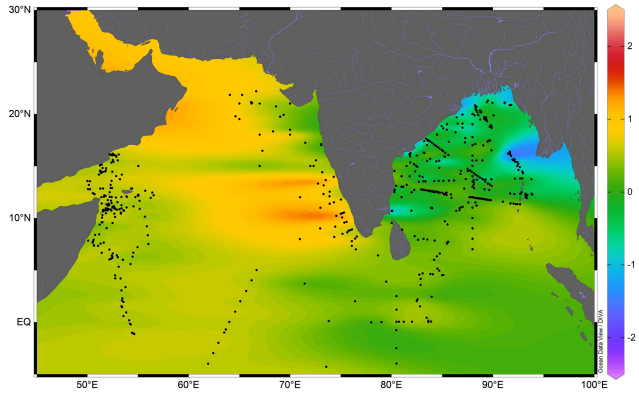

Figure 8. The surface seawater oxygen isotopic ratio (‰) in the northern Indian Ocean. The black-filled circles are the seawater sample locations compiled from previous studies. The thin blue lines are the major rivers draining in the northern Indian Ocean. The map was prepared by using Ocean Data View software (Schlitzer, 2018).

1971). The increase in $\delta^{18}O_{ruber}$ with depth is similar in both the Arabian Sea and BoB.

Additionally, the gradual decrease in the sedimentation rate with increasing depth and distance from the continental margins can also induce a depth-related trend in $\delta^{18}O_{ruber}$. The bioturbation disturbs the top few centimetres of the sediments (Gerino et al., 1998), mixing older shells with comparatively younger shells (Löwemark and Grootes, 2004). In high sedimentation rate regions of the shelf and slope, the mixing is restricted to the shells deposited in a shorter, climatologically stable interval. However, in the deeper regions, it is likely that the shells deposited during the colder glacial interval or deglaciation with relatively higher $\delta^{18}O_{ruber}$ are mixed with the younger shells, as these are available close to the surface due to the low sedimentation rate (Broecker, 1986; Anderson, 2001). The mixing of shells with a relatively higher $\delta^{18}O$ with the modern shells having lighter $\delta^{18}O$ can also result in the depth-related increasing trend of $\delta^{18}O_{ruber}$. The sedimentation rate is very high on the slope and decreases in the deeper regions of both the Arabian Sea

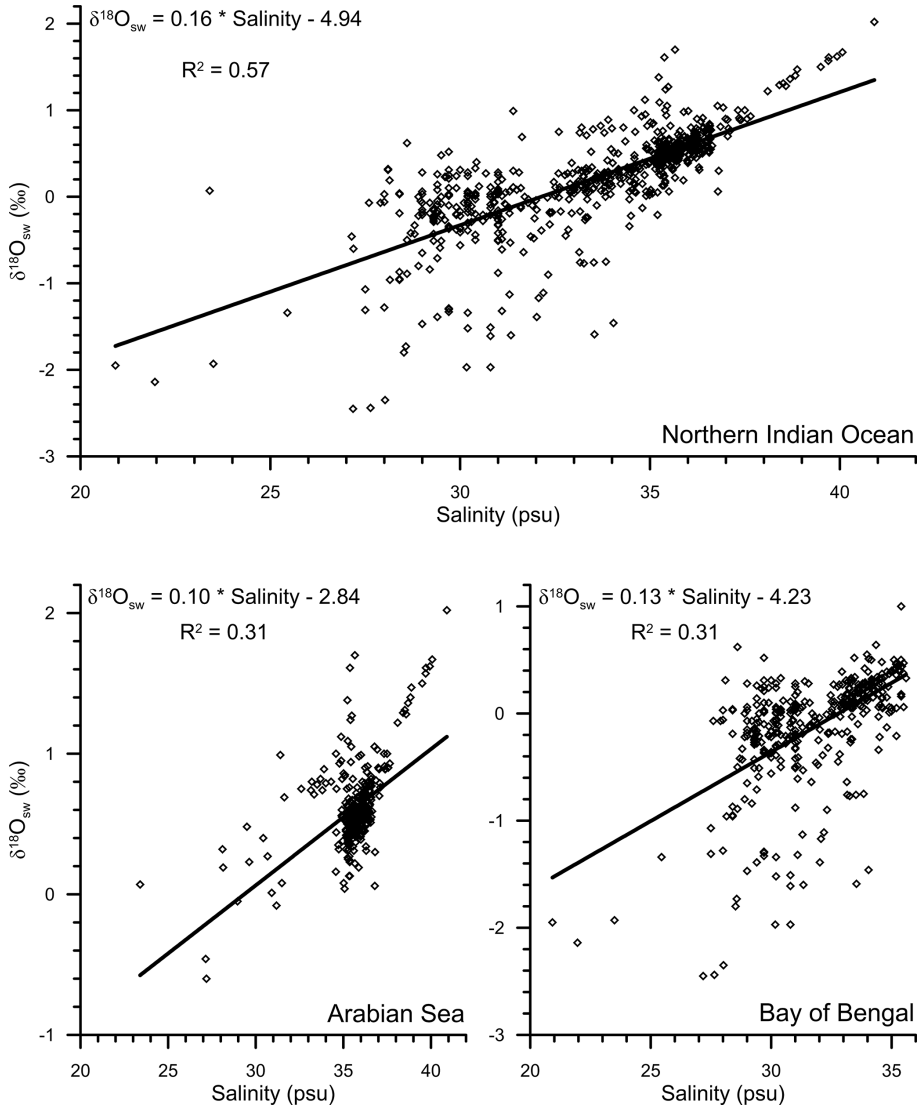

Figure 9. The relationship between the surface water oxygen isotopic ratio and salinity in the northern Indian Ocean (5° S–30° N), Arabian Sea, and the Bay of Bengal. The data points are from Schmidt et al. (1999), Delaygue et al. (2001), Singh et al. (2010), and Achyuthan et al. (2013).

(Singh et al., 2017) and BoB (e.g. Bhonsale and Saraswat, 2012; Suokhrie et al., 2022). However, it should be noted here that the sedimentation rate in large parts of the BoB is still high enough to prevent availability of deglacial or last glacial maximum shells within the bioturbation-induced mixing limits.

The large influence of the terrestrial freshwater influx in the shallower region, as compared to the deeper parts of the northern Indian Ocean, is also likely to contribute to the observed increase in $\delta^{18}O_{ruber}$ with depth. The freshwater is depleted in heavier oxygen isotopes as compared to the seawater (Bhattacharya et al., 1985; Ramesh and Sarin, 1992). Thus, the foraminiferal shells secreted in the shallow waters are likely to be enriched in the lighter oxygen isotope, resulting in a depth-related bias. Therefore, to delineate the influence of depth-related diagenetic alteration and secondary calcification in $\delta^{18}O_{ruber}$, we subtracted the expected $\delta^{18}O_{calcite}$ from the measured $\delta^{18}O_{ruber}$. The difference between the measured $\delta^{18}O_{ruber}$ and expected $\delta^{18}O_{calcite}$ was plotted with water depth (Fig. 12). The difference (measured $\delta^{18}O_{ruber}$ minus expected $\delta^{18}O_{calcite}$) increased with depth, suggesting a strong influence of the depth-related processes in $\delta^{18}O_{ruber}$.

6.4 Salinity contribution to $\delta^{18}O_{ruber}$

We report a strong influence of the freshwater-influx-induced salinity on $\delta^{18}O_{ruber}$ ($R^2 = 0.63$). As expected, $\delta^{18}O_{ruber}$ has a direct positive relationship with the ambient salinity. The $\delta^{18}O_{ruber}$ increased by 0.29 ‰ for every practical salinity

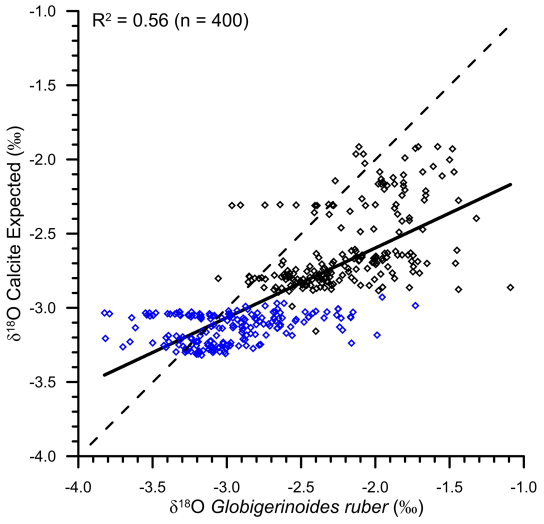

Figure 10. The scatterplot of expected δ^{18}O calcite (as estimated from the ambient salinity–temperature) and the analysed $\delta^{18}\mathbf{O_{ruber}}$. The two are significantly correlated ($R^2 = 0.56$), suggesting that *Globigerinoides ruber* correctly represents the ambient conditions. The blue diamonds are the samples collected from the Bay of Bengal, and the black diamonds represent the samples collected from the Arabian Sea. The dotted line represents the 1 : 1 relationship between the measured and expected δ^{18}O.

unit (psu) increase in salinity. The northern Indian Ocean has a large salinity gradient ($\sim$ 10 psu) from the lowest in the northern BoB to the highest in the northwestern Arabian Sea, which is mainly driven by the freshwater input. The river water and direct precipitation is enriched in the lighter oxygen isotope (Kumar et al., 2010; Kathayat et al., 2021). Thus, the increased riverine influx and precipitation contributes isotopically lighter water to the surface ocean (Rai et al., 2021) and decreases the $\delta^{18}O_{ruber}$. From the surface seawater samples collected during the winter monsoon season (January–February 1994), a δ^{18}O–salinity slope of 0.26 ‰ was deduced for the Arabian Sea and 0.18 ‰ for the BoB (Delaygue et al., 2001). However, the δ^{18}O–salinity slope also varies regionally during different seasons (Singh et al., 2010; Achyuthan et al., 2013). The δ^{18}O–salinity slope varied from as low as 0.10 for the coastal BoB samples collected during the months of April–May to as high as 0.51 for the samples collected from the western BoB during the peak southwestern monsoon season (August–September 1988; Singh et al., 2010). The large seasonal variation implies limitations in the δ^{18}O–salinity slope deduced from snapshot surface seawater samples. Additionally, *G. ruber* flux is reported throughout the year (Guptha et al., 1997), suggesting that the fossil population represents annual average conditions (Thirumalai et al., 2014).

A different $\delta^{18}O_{ruber}$–salinity slope for the Arabian Sea (0.28) and BoB (0.19) is attributed to the different hydrographic regimes of these two basins. The runoff and precipitation excess in the BoB results in a comparatively lower salinity as compared to the evaporation-dominated Arabian Sea. However, it should be noted here that the relationship between $\delta^{18}O_{ruber}$ and salinity was very robust for all of the northern Indian Ocean samples plotted together. Interestingly, the slope of δ^{18}O–salinity for the entire northern Indian Ocean samples is much lower than that for the Atlantic Ocean (0.59 for the North Atlantic and 0.52 for the South Atlantic; Delaygue et al., 2000), despite the large meltwater influx into the North Atlantic. The dissimilar δ^{18}O–salinity slope in different basins and also during different seasons in the same basin is mainly attributed to the variation in the end-member composition and the relative amount of freshwater (riverine/precipitation/sub-marine groundwater discharge) input from various sources during different seasons (Achyuthan et al., 2013; Tiwari et al., 2013). The heavier oxygen-isotope-depleted precipitation/freshwater influx in the higher latitudes (~ -35 ‰) as compared to the tropical areas (~ -5 ‰) also results in a higher slope of the δ^{18}O–salinity relationship in the North Atlantic Ocean (Rozanski et al., 1993). Additionally, the difference in the δ^{18}O–salinity slope despite the huge freshwater input into both the basins is also because a large fraction of the riverine freshwater spreads across the surface of the northern Indian Ocean, while the meltwater sinks to deeper depths in the North Atlantic Ocean. A consistent systematic difference has previously been observed between planktic foraminiferal shells collected in plankton tows and surface sediments, with shells from the sediments being comparatively enriched in ^{18}O (Vergnaud-Grazzini, 1976).

6.5 Temperature control on $\delta^{18}O_{ruber}$

A first-order comparison of the uncorrected $\delta^{18}O_{ruber}$ with ambient temperature of the top 30 m of the water column at respective stations showed 0.32 ‰ decrease with every 1 °C warming. The change in $\delta^{18}O_{ruber}$, as inferred from the core-top sediments of the northern Indian Ocean is higher than that estimated from the plankton tows (0.22 ‰ per 1 °C change in temperature; Mulitza et al., 2003). The seawater temperature was amongst the primary factors identified to affect $\delta^{18}O_{ruber}$ (Emiliani, 1954; Mulitza et al., 2003). The low correlation between $\delta^{18}O_{ruber}$ and temperature in this data set is attributed to the limited temperature variability (1, 28–29 °C) at a majority of the stations. The large salinity difference ($\sim$ 6.5 psu) between stations further obscures any significant correlation between uncorrected $\delta^{18}O_{ruber}$ and temperature. The temperature influence on $\delta^{18}O_{ruber}$ was thus assessed by comparing the ambient temperature with the $\delta^{18}O_{ruber}$ corrected for $\delta^{18}O_{sw}$ ($\delta^{18}O_{ruber} - \delta^{18}O_{sw}$). The pH of the seawater has also been identified as a factor affecting the stable oxygen isotopic composition of planktic foraminifera (Bijma et al., 1999). However, as argued by Mulitza et al. (2003), the limited modern surface seawater pH variability (Chakraborty et al., 2021) and its close dependence on temperature implies

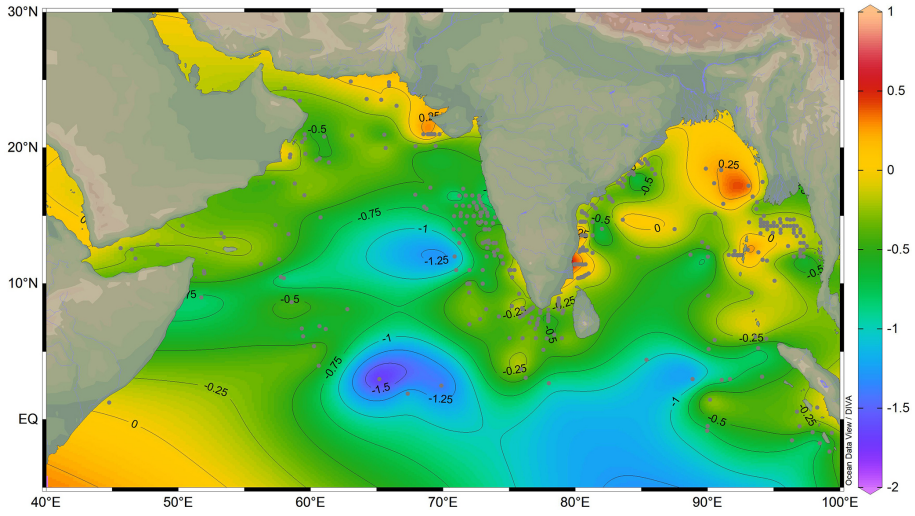

Figure 11. The difference in the expected $\delta^{18}O_{calcite}$ and observed $\delta^{18}O_{ruber}$ ($\delta^{18}O_{residual}$) in the surface sediments of the northern Indian Ocean. The grey-filled squares are the sample locations. The thin blue lines are the major rivers draining in the northern Indian Ocean. The thin black lines mark the contours at 0.25 ‰ intervals. The map was prepared by using Ocean Data View software (Schlitzer, 2018).

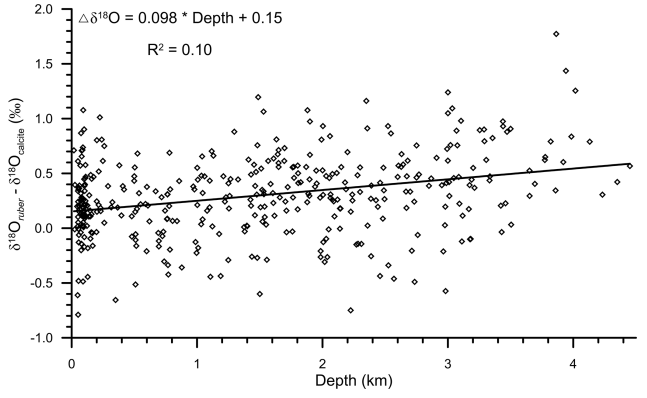

Figure 12. The relationship of the difference between measured $\delta^{18}O_{ruber}$ and expected $\delta^{18}O_{calcite}$ with the water depth from which the surface samples were collected in the northern Indian Ocean. The $\delta^{18}O_{ruber} - \delta^{18}O_{calcite}$ increased with increasing water depth.

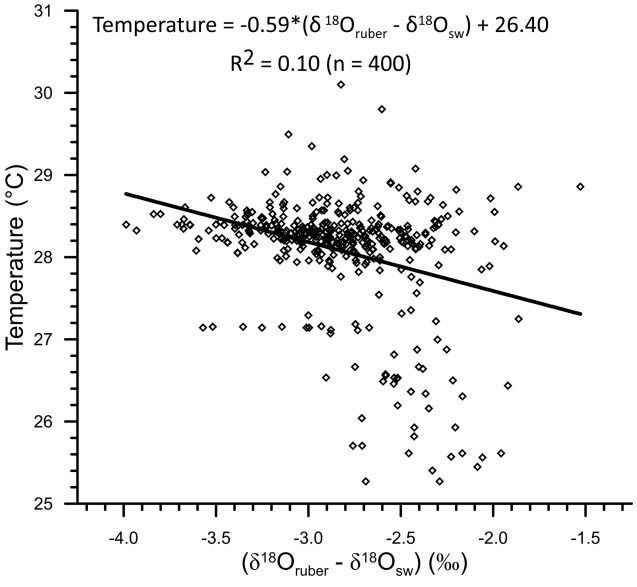

Figure 13. The relationship between ambient temperature and ($\delta^{18}O_{ruber} - \delta^{18}O_{sw}$) for the northern Indian Ocean. As expected, the ($\delta^{18}O_{ruber} - \delta^{18}O_{sw}$) becomes enriched in heavier isotopes with decreasing ambient temperature.

that the pH contribution to $\delta^{18}O_{ruber}$ is well within the error associated with the measurements. The seawater pH in the immediate vicinity of the foraminiferal shell is strongly influenced by the light intensity in the presence of symbionts (Jørgensen et al., 1985). The riverine influx in the northern Indian Ocean makes the surface waters turbid, reducing the light penetration depths (Prasanna Kumar et al., 2010). Therefore, riverine-influx-induced variations in turbidity in the northern Indian Ocean can influence the $\delta^{18}O_{ruber}$ via the pH effect.

The comparison of $\delta^{18}O_{sw}$-corrected $\delta^{18}O_{ruber}$ with the ambient temperature also confirms the enrichment of ($\delta^{18}O_{ruber} - \delta^{18}O_{sw}$) in heavier oxygen isotope with the decrease in temperature (Fig. 13). We obtained the following relationship between temperature and ($\delta^{18}O_{ruber} - \delta^{18}O_{sw}$) in the northern Indian Ocean.

$$\text{Temperature} = -0.59 \cdot (\delta^{18}O_{ruber} - \delta^{18}O_{sw}) + 26.40. \quad (1)$$

The slope of the temperature and ($\delta^{18}O_{ruber} - \delta^{18}O_{sw}$) was somewhat different (0.17 ‰ 1 °C change in temperature) than that of the temperature versus uncorrected $\delta^{18}O_{ruber}$ but similar to that reported for the plankton tows (0.22 ‰ 1 °C change in temperature; Mulitza et al., 2003).

7 Data availability

The newly generated data and the data compiled from previous studies from the northern Indian Ocean have been submitted to PANGAEA and are available at https://doi.org/10.1594/PANGAEA.945401 (Saraswat et al., 2022). These data are also available in the Supplement of this article.

8 Conclusions

We measured the stable oxygen isotopic ratio of the surface-dwelling planktic foraminifera *Globigerinoides ruber* (white variety) from the surface sediments of the northern Indian Ocean. A comparison of the $\delta^{18}O_{ruber}$ with the depth suggests a strong diagenetic alteration of the isotopic ratio. The freshwater-influx-induced changes in the ambient salinity exert the maximum influence on the $\delta^{18}O_{ruber}$, suggesting its robust application for reconstructing the past salinity in the northern Indian Ocean. The large east–west salinity gradient in the northern Indian Ocean results in a strong longitudinal variation in $\delta^{18}O_{ruber}$. The temperature influence on $\delta^{18}O_{ruber}$ is subdued as compared to the effect of large salinity variation in the northern Indian Ocean. We report a relatively smaller change in $\delta^{18}O_{ruber}$ with a unit increase in ambient temperature in case of specimens retrieved from the surface sediments as compared to those collected live from the water column.

Supplement. The supplement related to this article is available online at: https://doi.org/10.5194/essd-15-171-2023-supplement.

Author contributions. RS designed the research, compiled and interpreted the data, and wrote the paper. TS, DKN, DPS, SMS, MS, GK, SRB, and SRK picked the specimens for isotopic analysis. MM and ASM supervised the analysis. All authors edited and contributed to the final version of this work.

Competing interests. The contact author has declared that none of the authors has any competing interests.

Disclaimer. Publisher's note: Copernicus Publications remains neutral with regard to jurisdictional claims in published maps and institutional affiliations.

Acknowledgements. We thank the crew on board expeditions during which the surface sediment samples were collected. The authors thank the director of the CSIR-National Institute of Oceanography, for the facilities and funding. The technical personnel at the Alfred Wegener Institute for Polar and Marine Research and MARUM, Bremen University, Germany, are acknowledged, for their help in the stable isotopic analysis. We thank Prattipati Subba Rao and Venkitasubramani Ramaswamy, CSIR-NIO, for providing the surface sediment samples collected from the Myanmar continental shelf. The authors also thank Bejugam Nagender Nath, for providing the spade core-top samples from the eastern margin of India. We thank Alberto Sanchez, Centro Interdisciplinario de Ciencias Marinas, Instituto Politécnico Nacional, La Paz, B. C. S, Mexico, and the anonymous reviewer, for their constructive comments and suggestions that helped to improve the paper.

Financial support. This research has been supported by the Council of Scientific and Industrial Research, India (LEMAP).

Review statement. This paper was edited by Giuseppe M. R. Manzella and reviewed by Alberto Sanchez and one anonymous referee.

References

Achyuthan, H., Deshpande, R. D., Rao, M. S., Kumar, B., Nallathambi, T., Shashi Kumar, K., Ramesh, R., Ramachandran, P., Maurya, A. S., and Gupta, S. K.: Stable isotopes and salinity in the surface waters of the Bay of Bengal: Implications for water dynamics and palaeoclimate, Mar. Chem., 149, 51–62, 2013.

Anderson, D. M.: Attenuation of millennial-scale events by bioturbation in marine sediments, Paleoceanography, 16, 352–357, 2001.

Bé, A. W. H. and Hutson, W. H.: Ecology of planktonic foraminifera and biogeographic patterns of life and fossil assemblages in the Indian Ocean, Micropaleontology, 23, 369–414, 1977.

Bemis, B. E., Spero, H. J., Bijma, J., and Lea, D. W.: Reevaluation of the oxygen isotopic composition of planktonic foraminifera: Experimental results and revised paleotemperature equations, Paleoceanography, 13, 150–160, 1998.

Berger, W. H.: Sedimentation of planktonic foraminifera, Mar. Geol., 11, 325–358, 1971.

Berger, W. H. and Gardner, J. V.: On the determination of Pleistocene temperatures from planktonic foraminifera, J. Foram. Res. 5, 102–113, 1975.

Berger, W. H. and Killingley, J. S.: Glacial-Holocene transition in deep-sea carbonates: selective dissolution and the stable isotope signal, Science, 197, 563–566, 1977.

Bhadra, S. R. and Saraswat, R.: Assessing the effect of riverine discharge on planktic foraminifera: A case study from the marginal marine regions of the western Bay of Bengal, Deep-Sea Res. Pt. II, 183, 104927, https://doi.org/10.1016/j.dsr2.2021.104927, 2021.

Bhattacharya, S. K., Gupta, S. K., and Krishnamurthy, R. V.: Oxygen and hydrogen isotopic ratios in ground waters and river waters from India, Proc. Indian Acad. Sci. (Earth Planet. Sci.), 94, 283–295, 1985.

Bhonsale, S. and Saraswat, R.: Abundance and size variation of *Globorotalia menardii* in the northeastern Indian Ocean during the late Quaternary, J. Geol. Soc. India, 80, 771–782, 2012.

Bijma, J., Spero, H. J., and Lea, D. W.: Reassessing foraminiferal stable isotope geochemistry: Impact of the oceanic carbonate system (experimental results), in: Use of Proxies in Paleoceanography: Examples from the South Atlantic, edited by: Fischer, G. and Wefer, G., Springer, Berlin, pp. 489–512, 1999.

Bonneau, M.-C., Vergnaud-Grazzini, C., and Berger, W. H.: Stable isotope fractionation and differential dissolution in Recent planktonic foraminifera from Pacific box-cores, Oceanol. Ac., 3, 377–382, 1980.

Boyer, T. P., Antonov, J. I., Baranova, O. K., Garcia, H. E., Johnson, D. R., Mishonov, A. V., O'Brien, T. D., Paver, C. R., Reagan, J. R., Seidov, D., Smolyar, I. V., and Zweng, M. M.: edited by: Levitus, S., and Mishonov, A.: NOAA Atlas NESDIS 72, World Ocean Database, 209 pp., https://doi.org/10.7289/V5NZ85MT, 2013.

Bristow, L. A., Callbeck, C. M., Larsen, M., Altabet, M. A., Dekaezemacker, J., Forth, M., Gauns, M., Glud, R. N., Kuypers, M. M. M., Lavik, G., Milucka, J., Naqvi, S. W. A., Pratihary, A., Revsbech, N. P., Thamdrup, B., Treusch, A. H., and Canfield, D. E.: N_2 production rates limited by nitrite availability in the Bay of Bengal oxygen minimum zone, Nat. Geosci., 10, 24–29, 2017.

Broecker, W. S.: Oxygen isotope constraints on surface ocean temperatures, Quat. Res., 26, 121–134, https://doi.org/10.1016/0033-5894(86)90087-6, 1986.

Chaitanya, A. V. S., Lengaigne, M., Vialard, J., Gopalakrishna, V. V., Durand, F., Kranthikumar, C., Amritash, S., Suneel, V., Papa, F., and Ravichandran, M.: Salinity measurements collected by fishermen reveal a "river in the sea" flowing along the eastern coast of India, B. Am Meteorol. Soc., 95, 1897–1908, 2014.

Chakraborty, K., Valsala, V., Bhattacharya, T., and Ghosh, J.: Seasonal cycle of surface ocean pCO_2 and pH in the northern Indian Ocean and their controlling factors, Progr. Oceanogra., 198, 102683, https://doi.org/10.1016/j.pocean.2021.102683, 2021.

Chatterjee, A., Kumar, B. P., Prakash, S., and Singh, P.: Annihilation of the Somali upwelling system during summer monsoon, Sci. Rep.-UK, 9, 1–14, 2019.

Dämmer, L. K., de Nooijer, L., van Sebille, E., Haak, J. G., and Reichart, G.-J.: Evaluation of oxygen isotopes and trace elements in planktonic foraminifera from the Mediterranean Sea as recorders of seawater oxygen isotopes and salinity, Clim. Past, 16, 2401–2414, https://doi.org/10.5194/cp-16-2401-2020, 2020.

De Deckker, P.: The Indo-Pacific Warm Pool: critical to world oceanography and world climate, Geosci. Lett., 3, 20, https://doi.org/10.1186/s40562-016-0054-3, 2016.

Delaygue, G., Jouzel, J., and Dutay, J. C.: Oxygen 18–salinity relationship simulated by an oceanic general circulation model, Earth Planet. Sc. Lett., 178, 113–123, 2000.

Delaygue, G., Bard, E., Rollion, C., Jouzel, J., Stievenard, M., and Duplessy, J.-C.: Oxygen isotope/salinity relationship in the northern Indian Ocean, J. Geophys. Res., 106, 4565–4574, 2001.

Duplessy, J. C.: Glacial to interglacial contrasts in the northern Indian Ocean, Nature, 295, 494–498, 1982.

Duplessy, J. C., Bé, A. W. H., and Blanc, P. L.: Oxygen and carbon isotopic composition and biogeographic distribution of planktonic foraminifera in the Indian Ocean, Palaeogeogr. Palaeocl., 33, 9–46, 1981a.

Duplessy, J. C., Blanc, P. L., and Bé, A. W. H.: Oxygen-18 enrichment of planktonic foraminifera due to gametogenic calcification below the euphotic zone, Science, 213, 1247–1250, 1981b.

Emiliani, C.: Depth habitat of some species of pelagic foraminifera as indicated by oxygen isotope ratio, Am. J. Sci., 252, 149–158, 1954.

Fairbanks, R. G. and Wiebe, P. H.: Foraminifera and chlorophyll maximum: vertical distribution, seasonal succession, and paleoceanographic significance, Science, 209, 1524–1526, https://doi.org/10.1126/science.209.4464.1524, 1980.

Farmer, E. C., Kaplan, A., de Menocal, P. B., and Lynch-Stieglitz, J.: Corroborating ecological depth preferences of planktonic foraminifera in the tropical Atlantic with the stable oxygen isotope ratios of core top specimens, Paleoceanography, 22, PA3205, https://doi.org/10.1029/2006PA001361, 2007.

Fraile, I., Schulz, M., Mulitza, S., and Kucera, M.: Predicting the global distribution of planktonic foraminifera using a dynamic ecosystem model, Biogeosciences, 5, 891–911, https://doi.org/10.5194/bg-5-891-2008, 2008.

Ganssen, G. and Kroon, D.: Evidence for Red Sea surface water circulation from oxygen isotopes of modern surface waters and planktonic foraminiferal tests, Paleoceanography, 6, 73–82, 1991.

Gerino, M., Aller, R. C., Lee, C., Cochran, J. K., Aller, J. Y., Green, M. A., and Hirschberg, D.: Comparison of different tracers and methods used to quantify bioturbation during a spring bloom: 234-Thorium, luminophores and chlorophyll *a*, Estuarine Coast. Shelf Sci., 46, 531–547, 1998.

Guptha, M. V. S., Curry, W. B., Ittekkot, V., and Muralinath, A. S.: Seasonal variation in the flux of planktic foraminifera: Sediment trap results from the Bay of Bengal, northern Indian Ocean, J. Foraminiferal Res., 27, 5–19, 1997.

Hemleben, C., Spindler, M., and Anderson, O. R.: Modern Planktonic Foraminifera, Springer-Verlag, New York, https://doi.org/10.1007/978-1-4612-3544-6, 1989.

Hollstein, M., Mohtadi, M., Rosenthal, Y., Moffa Sanchez, P., Oppo, D., Martínez Méndez, G., Steinke, S., and Hebbeln, D.: Stable oxygen isotopes and Mg/Ca in planktic foraminifera from modern surface sediments of the Western Pacific Warm Pool: Implications for thermocline reconstructions, Paleoceanography, 32, 1174–1194, 2017.

Horikawa, K., Kodaira, T., Zhang, J., and Murayama, M.: $\delta^{18}O_{sw}$ estimate for *Globigerinoides ruber* from core-top sediments in the East China Sea, Progr. Earth Planet. Sci., 2, 19, https://doi.org/10.1186/s40645-015-0048-3, 2015.

Howden, S. D. and Murtugudde, R.: Effects of river inputs into the Bay of Bengal, J. Geophys. Res., 106, 19825–19844, 2001.

Hut, G.: Consultants group meeting on stable isotope reference samples for geochemical and hydrological investigations, Report to the Director General, International Atomic Energy Agency, Vienna, 42 pp., 1987.

Jørgensen, B. B., Erez, J., Revsbech, P., and Cohen, Y.: Symbiotic photosynthesis in a planktonic foraminiferan, *Globigerinoides sacculifer* (Brady), studied with microelectrodes, Limnol. Oceanogr., 30, 1253–1267, 1985.

Joseph, S. and Freeland, H. J.: Salinity variability in the Arabian Sea, Geophys. Res. Lett., 32, L09607, https://doi.org/10.1029/2005GL022972, 2005.

Kallel, N., Paterne, M., Duplessy, J., Vergnaudgrazzini, C., Pujol, C., Labeyrie, L., Arnold, M., Fontugne, M., and Pierre, C.: Enhanced rainfall in the Mediterranean region during the last Sapropel Event, Oceanol. Ac., 20, 697–712, 1997.

Kathayat, G., Sinha, A., Tanoue, M., Yoshimura, K., Li, H., Zhang, H., and Cheng, H.: Interannual oxygen isotope variability in Indian summer monsoon precipitation reflects changes in moisture sources, Comm. Earth Environ., 2, 96, https://doi.org/10.1038/s43247-021-00165-z, 2021.

Kemle-von-Mücke, S. and Hemleben, C.: Planktic Foraminifera, in: South Atlantic zooplankton, edited by: Boltovskoy, E., Backhuys Publishers, Leiden, 43–67, 1999.

Kessarkar, P. M., Purnachadra Rao, V., Naqvi, S. W. A., and Karapurkar, S. G.: Variation in the Indian summer monsoon intensity during the Bølling-Ållerød and Holocene, Paleoceanography, 28, 413–425, 2013.

Kroon, D. and Ganssen, G.: Northern Indian Ocean upwelling cells and the stable isotope composition of living planktonic foraminifers, Deep-Sea Res., 36, 1219–1236, 1989.

Kumar, B., Rai, S. P., Saravana Kumar, U., Verma, S. K., Garg, P., Vijaya Kumar, S. V., Jaiswal, R., Purendra, B. K., Kumar, S. R., and Pande, N. G.: Isotopic characteristics of Indian precipitation, Water Resource Res., 46, W12548, https://doi.org/10.1029/2009WR008532, 2010.

Lambeck, K., Rouby, H., Purcell, A., Sun, Y., and Sambridge, M.: Sea level and global ice volumes from the Last Glacial Maximum to the Holocene, P. Natl. Acad. Sci. USA, 111, 15296–15303, 2014.

Lea, D. W.: Elemental and isotopic proxies of past ocean temperatures, Treatise Geochem., 8, 373–397, 2014.

Locarnini, R. A., Mishonov, A. V., Baranova, O. K., Boyer, T. P., Zweng, M. M., Garcia, H. E., Reagan, J. R., Seidov, D., Weathers, K., Paver, C. R., and Smolyar, I.: World Ocean Atlas 2018, Volume 1: Temperature, edited by: Mishonov, A., NOAA Atlas NESDIS 81, 52 pp., 2018.

Lohmann, G. P.: A model for variation in the chemistry of planktonic foraminifera due to secondary calcification and selective dissolution, Paleoceanography, 10, 445–457, 1995.

Löwemark, L. and Grootes, P. M.: Large age differences between planktic foraminifers caused by abundance variations and Zoophycos bioturbation, Paleoceanography, 19, PA2001, https://doi.org/10.1029/2003PA000949, 2004.

Löwemark, L., Hong, W.-L., Yui, T.-F., and Hung, G.-W.: A test of different factors influencing the isotopic signal of planktonic foraminifera in surface sediments from the northern South China Sea, Mar. Micropaleontol., 55, 49–62, 2005.

Madhu, N. V., Jyothibabu, R., Maheswaran, P. A., Gerson, V. J., Gopalakrishnan, T. C., and Nair, K. K. C.: Lack of seasonality in phytoplankton standing stock (chlorophyll *a*) and production in the western Bay of Bengal, Cont. Shelf Res., 26, 1868–1883, 2006.

Madhupratap, M., Kumar, S. P., Bhattathiri, P. M. A., Kumar, M. D., Raghukumar, S., Nair, K. K. C., and Ramaiah, N.: Mechanism of the biological response to winter cooling in the northeastern Arabian Sea, Nature, 384, 549–552, 1996.

Mahesh, B. S. and Banakar, V. K.: Change in the intensity of low-salinity water inflow from the Bay of Bengal into the Eastern Arabian Sea from the Last Glacial Maximum to the Holocene: Implications for monsoon variations, Palaeogeogr. Palaeocl., 397, 31–37, 2014.

McCorkle, D. C., Martin, P. A., Lea, D. W., and Klinkhammer, G. P.: Evidence of a dissolution effect on benthic foraminiferal shell chemistry: δ^{13}C, Cd/Ca, Ba/Ca, and Sr/Ca results from the Ontong Java Plateau, Paleoceanography, 10, 699–714, 1997.

Metcalfe, B., Feldmeijer, W., and Ganssen, G. M.: Oxygen isotope variability of planktonic foraminifera provide clues to past upper ocean seasonal variability, Paleoceanogr. Paleocl., 34, 374–393, 2019.

Mohtadi, M., Oppo, D. W., Lückge, A., DePol-Holz, R., Steinke, S., Groeneveld, J., Hemme, N., and Hebbeln, D.: Reconstructing the thermal structure of the upper ocean: Insights from planktic foraminifera shell chemistry and alkenones in modern sediments of the tropical eastern Indian Ocean, Paleoceanography, 26, PA3219, https://doi.org/10.1029/2011PA002132, 2011.

Mulitza, S., Dürkoop, A., Hale, W., Wefer, G., and Niebler, H. S.: Planktonic foraminifera as recorders of past surface-water stratification, Geology, 25, 335–338, 1997.

Mulitza, S., Wolff, T., Pätzold, J., Hale, W., and Wefer, G.: Temperature sensitivity of planktic foraminifera and its influence on the oxygen isotope record, Mar. Micropaleontol., 33, 223–240, 1998.

Mulitza, S., Boltovskoy, D., Donner, B., Meggers, H., Paul, A., and Wefer, G.: Temperature:δ^{18}O relationships of planktonic foraminifera collected from surface waters, Palaeogeogr. Palaeocl., 202, 143–152, 2003.

Naqvi, S. W. A.: Deoxygenation in marginal seas of the Indian Ocean, Front. Mar. Sci., 8, 624322, https://doi.org/10.3389/fmars.2021.624322, 2021.

Naqvi, S. W. A., Naik, H., Pratihary, A., D'Souza, W., Narvekar, P. V., Jayakumar, D. A., Devol, A. H., Yoshinari, T., and Saino, T.: Coastal versus open-ocean denitrification in the Arabian Sea, Biogeosciences, 3, 621–633, https://doi.org/10.5194/bg-3-621-2006, 2006.

Narvekar, J. and Prasanna Kumar, S.: Mixed layer variability and chlorophyll a biomass in the Bay of Bengal, Biogeosciences, 11, 3819–3843, https://doi.org/10.5194/bg-11-3819-2014, 2014.

Panchang, R. and Nigam, R.: High resolution climatic records of the past ∼ 489 years from Central Asia as derived from benthic foraminiferal species, *Asterorotalia trispinosa*, Mar. Geol., 307, 88–104, 2012.

Pearson, P. N.: Oxygen isotopes in foraminifera: Overview and historical review, in: Reconstructing Earth's Deep-Time Climate – The State of the Art in 2012, Paleontological Society Short Course, 3 November 2012, The Paleontological Society Papers, vol. 18, edited by: Ivany, L. C. and Huber, B. T., 1–38, 2012.

Prasanna Kumar, S. and Prasad, T. G.: Formation and spreading of Arabian Sea high-salinity water mass, J. Geophys. Res.-Oceans, 104, 1455–1464, 1999.

Prasanna Kumar, S., Nuncio, M., Narvekar, J., Kumar, A., Sardesai, D. S., De Souza, S. N., Gauns, M., Ramaiah, N., and Madhupratap, M.: Are eddies nature's trigger to enhance biological productivity in the Bay of Bengal?, Geophys. Res. Lett., 31, L07309, https://doi.org/10.1029/2003GL019274, 2004.

Prasanna Kumar, S., Narvekar, J., Nuncio, M., Gauns, M., and Sardesai, S.: What drives the biological productivity of the northern Indian Ocean?, Washington D.C. American Geophysical Union Geophysical Monograph Series, 185, 33–56, 2009.

Prasanna Kumar, S., Narvekar, J., Nuncio, M., Kumar, A., Ramaiah, N., Sardesai, S., Gauns, M., Fernandes, V., and Paul J.: Is the biological productivity in the Bay of Bengal light limited?, Curr. Sci., 98, 1331–1339, 2010.

Prell, W. L. and Curry, W. B.: Faunal and isotopic indices of monsoonal upwelling: Western Arabian Sea, Oceanol. Ac., 4, 91–98, 1981.

Qasim, S. Z.: Biological productivity of the Indian Ocean, Indian J. Mar. Sci., 6, 122–137, 1977.

Rai, S. P., Noble, J., Singh, D., Rawat, Y. S., and Kumar, B.: Spatiotemporal variability in stable isotopes of the Ganga River and factors affecting their distributions, Catena, 204, 105360, https://doi.org/10.1016/j.catena.2021.105360, 2021.

Ramaswamy, V., Gaye, B., Shirodkar, P. V., Rao, P. S., Chivas, A. R., Wheeler, D., and Thwin, S.: Distribution and sources of organic carbon, nitrogen and their isotopic signatures in sediments from the Ayeyarwady (Irrawaddy) continental shelf, northern Andaman Sea, Mar. Chem., 111, 137–150, 2008.

Ramesh, R. and Sarin, M. M.: Stable isotope study of the Ganga (Ganges) river system, J. Hydrology, 139, 49–62, 1992.

Rao, R. R. and Sivakumar, R.: Seasonal variability of sea surface salinity and salt budget of the mixed layer of the northIndian Ocean, J. Geophys. Res., 108, 3009, https://doi.org/10.1029/2001JC000907, 2003.

Rixen, T., Cowie, G., Gaye, B., Goes, J., do Rosário Gomes, H., Hood, R. R., Lachkar, Z., Schmidt, H., Segschneider, J., and Singh, A.: Reviews and syntheses: Present, past, and future of the oxygen minimum zone in the northern Indian Ocean, Biogeosciences, 17, 6051–6080, https://doi.org/10.5194/bg-17-6051-2020, 2020.

Rochford, D. J.: Salinity maximum in the upper 100 meters of the north Indian Ocean, Aust. J. Mar. Freshwater Res., 15, 1–24, 1964.

Rozanski, K., Araguás-Araguás, L., and Gonfiantini, R.: Isotopic Patterns in Modern Global Precipitation, in: Climate Change in Continental Isotopic Records, edited by: Swart, P. K., Lohmann, K. C., Mckenzie, J., and Savin, S., American Geophysical Union, Washington, D.C., 1–36, https://doi.org/10.1029/GM078p0001, 1993.

Saalim, S. M., Saraswat, R., and Nigam, R.: Ecological preferences of living benthic foraminifera from the Mahanadi river-dominated north-western Bay of Bengal: A potential environmental impact assessment tool, Mar. Poll. Bull., 175, 113158, https://doi.org/10.1016/j.marpolbul.2021.113158, 2022.

Sánchez, A., Sánchez-Vargas, L., Balart, E., and Domínguez-Samalea, Y.: Stable oxygen isotopes in planktonic foraminifera from surface sediments in the California Current system, Mar. Micropaleontol., 173, 102127, https://doi.org/10.1016/j.marmicro.2022.102127, 2022.

Saraswat, R., Nigam, R., Mackensen, A., and Weldeab, S.: Linkage between seasonal insolation gradient in the tropical northern hemisphere and the sea surface salinity of the equatorial Indian Ocean during the last glacial period, Acta Geol. Sinica, 86, 801–811, 2012.

Saraswat, R., Lea, D. W., Nigam, R., Mackensen, A., and Naik, D. K.: Deglaciation in the tropical Indian Ocean driven by interplay between the regional monsoon and global teleconnections, Earth Planet. Sc. Lett., 375, 166–175, 2013.

Saraswat, R., Singh, D. P., Lea, D. W., Mackensen, A., and Naik, D. K.: Indonesian throughflow controlled the westward extent of the Indo-Pacific Warm Pool during glacial-interglacial intervals, Global Planet. Changes, 183, 103031, https://doi.org/10.1016/j.gloplacha.2019.103031, 2019.

Saraswat, R., Suokhrie, T., Naik, D. K., Singh, D. P., Saalim, S. M., Salman, M., Kumar, G., Bhadra, S. R., Mohtadi, M., Kurtarkar, S. R., and Maurya, A. S.: Oxygen isotopic ratio of *Globigerinoides ruber* (white variety) in the surface sediments of the northern Indian Ocean, PANGAEA [data set], https://doi.org/10.1594/PANGAEA.945401, 2022.

Sarma, V. V. and Aswanikumar, V.: Subsurface chlorophyll maxima in the north-western Bay of Bengal, J. Plankton Res., 11, 339–352, 1991.

Sarma, V. V. S. S., Chopra, M., Rao, D. N., Priya, M. M. R., Rajula, G. R., Lakshmi, D. S. R., and Rao, V. D.: Role of eddies on controlling total and size-fractionated primary production in the Bay of Bengal, Cont. Shelf Res., 204, 104186, https://doi.org/10.1016/j.csr.2020.104186, 2020.

Schlitzer, R.: Ocean Data View, https://odv.awi.de (last access: 5 November 2022), 2018.

Schmidt, G. A., Bigg, G. R., and Rohling, E. J.: Global Seawater Oxygen-18 Database – v1.22, https://data.giss.nasa.gov/o18data/ (last access: 30 October 2021), 1999.

Schmidt, M. W., Spero, H. J., and Lea, D. W.: Links between salinity variation in the Caribbean and North Atlantic thermohaline circulation, Nature, 428, 160–163, 2004.

Schrag, D. P., DePaolo, D. J., Richter, F. M.: Reconstructing past sea surface temperatures: Correcting for diagenesis of bulk marine carbonate, Geochim. Cosmochim. Ac., 59, 2265–2278, 1995.

Sengupta, D., Bharath Raj, G. N., and Shenoi, S. S. C.: Surface freshwater from Bay of Bengal runoff and Indonesian Throughflow in the tropical Indian Ocean, Geophys. Res. Lett., 33, L22609, https://doi.org/10.1029/2006GL027573, 2006.

Shackleton, N. J.: Oxygen isotopes, ice volume and sea level, Quaternay Sci. Rev., 6, 183–190, 1987.

Shackleton, N. J.: The 100,000-year Ice-Age cycle identified and found to lag temperature, carbon dioxide, and orbital eccentricity, Science, 289, 1897–1902, 2000.

Shackleton, N. J. and Vincent, E.: Oxygen and carbon isotope studies in recent foraminifera from the southwest Indian ocean, Mar. Micropaleontol., 3, 1–13, https://doi.org/10.1016/0377-8398(78)90008-7, 1978.

Shankar, D., Vinayachandran, P. N., and Unnikrishnan, A. S.: The monsoon currents in the north Indian Ocean, Progr. Oceanogr., 52, 63–120, 2002.

Shetye, S. R., Shenoi, S. S. C., Gouveia, A. D., Michael, G. S., Sundar, D., and Nampoothiri, G.: Wind-driven coastal upwelling along the western boundary of the Bay of Bengal during the southwest monsoon, Cont. Shelf Res., 11, 1397–1408, 1991.

Shetye, S. R., Gouveia, A. D., and Shenoi, S. S. C.: Circulation and water masses of the Arabian Sea, Proc. Indian Acad. Sci. (Earth Planet. Sci.), 103, 107–123, 1994.

Singh, A., Jani, R. A., and Ramesh, R.: Spatiotemporal variations of the δ^{18}O–salinity relation in the northern Indian Ocean, Deep-Sea Res. Pt. I, 57, 1422–1431, 2010.

Singh, D. P., Saraswat, R., and Naik, D. K.: Does glacial-interglacial transition affect sediment accumulation in monsoon dominated regions?, Acta Geol. Sinica, 91, 1079–1094, 2017.

Singh, D. P., Saraswat, R., and Nigam, R.: Untangling the effect of organic matter and dissolved oxygen on living benthic foraminifera in the southeastern Arabian Sea, Mar. Poll. Bull., 172, 112883, https://doi.org/10.1016/j.marpolbul.2021.112883, 2021.

Sirocko, F.: Zur Akkumulation von Staubsedimenten im nördlichen Indischen Ozean, Anzeiger der Klimageschichte Arabiens und Indiens. Dissertation, Berichte-Reports, Geologisch-Paläontologisches Institut der Universität Kiel, 27, 185 pp., 1989.

Smitha, A., Joseph, K. A., Jayaram, C., and Balchand, A. N.: Upwelling in the southeastern Arabian Sea as evidenced by Ekman mass transport using wind observations from OCEANSAT–II Scatterometer, Indian J. Geo-Mar. Sci., 43, 111–116, 2014.

Spero, H. J., Bijma, J., Lea, D. W., and Bemis, B. B.: Effect of seawater carbonate concentration on foraminiferal carbon and oxygen isotopes, Nature, 390, 497–500, 1997.

Sridevi, B. and Sarma, V. V. S. S.: A revisit to the regulation of oxygen minimum zone in the Bay of Bengal, J. Earth Syst. Sci., 129, 1–7, 2020.

Stainbank, S., Kroon, D., Rüggeberg, A., Raddatz, J., de Leau, E. S., Zhang, M., and Spezzaferri, S.: Controls on planktonic foraminifera apparent calcification depths for the northern equatorial Indian Ocean, PLoS ONE 14, e0222299, https://doi.org/10.1371/journal.pone.0222299, 2019.

Steph, S., Regenberg, M., Tiedemann, R., Mulitza, S., and Nürnberg, D.: Stable isotopes of planktonic foraminifera from tropical Atlantic/Caribbean coretops: Implications for reconstructing upper ocean stratification, Mar. Micropaleontol., 71, 1–19, 2009.

Suokhrie, T., Saraswat, R., and Nigam, R.: Multiple ecological parameters affect living benthic foraminifera in the river-influenced west-central Bay of Bengal, Front. Mar. Sci., 8, 467, https://doi.org/10.3389/fmars.2021.656757, 2021.

Suokhrie, T., Saraswat, R., and Saju, S.: Strong solar influence on multi-decadal periodic productivity changes in the central-western Bay of Bengal, Quaternary Int., 629, 16–26, https://doi.org/10.1016/j.quaint.2021.04.015, 2022.

Thirumalai, K., Richey, J. N., Quinn, T. M., and Poore, R. Z.: *Globigerinoides ruber* morphotypes in the Gulf of Mexico: A test of null hypothesis, Sci. Rep.-UK, 4, 6018, https://doi.org/10.1038/srep06018, 2014.

Thompson, P. R., Bé, A. W. H., Duplessy, J.-C., and Shackleton, N. J.: Disappearance of pink-pigmented *Globigerinoides ruber* at 120,000 yr BP in the Indian and Pacific oceans, Nature, 280, 554–558, 1979.

Thunell, R., Tappa, E., Pride, C., and Kincaid, E.: Sea-surface temperature anomalies associated with the 1997–1998 El Niño recorded in the oxygen isotope composition of planktonic foraminifera, Geology, 27, 843, https://doi.org/10.1130/0091-7613(1999)027<0843:SSTAAW>2.3.CO;2, 1999.

Tiwari, M., Nagoji, S. S., Kartik, T., Drishya, G., Parvathy, R. K., and Rajan, S.: Oxygen isotope–salinity relationships of discrete oceanic regions from India to Antarctica vis-à-vis surface hydrological processes, J. Mar. Syst., 113–114, 88–93, 2013.

Urey, H. C.: The thermodynamic properties of isotopic substances, J. Chem. Soc., 12, 562–569, 1947.

Vergnaud-Grazzini, C.: Non-equilibrium isotopic compositions of shells of planktonic foraminifera in the Mediterranean Sea, Palaeogeogr. Palaeocl., 20, 263–276, 1976.

Vinayachandran, P. N. and Shetye, S. R.: The warm pool in the Indian Ocean, Proc. Indian Acad. Sci. (Earth Planet Sci.), 100, 165–175, 1991.

Waelbroeck, C., Mulitza, S., Spero, H., Dokken, T., Kiefer, T., and Cortijo, E.: A global compilation of late Holocene planktonic foraminiferal δ^{18}O: relationship between surface water temperature and δ^{18}O, Quaternay Sci. Rev., 24, 853–868, https://doi.org/10.1016/j.quascirev.2003.10.014, 2005.

Wang, L., Sarnthein, M., Duplessy, J.-C., Erlenkeuser, H., Jung, S., and Pflaumann, U.: Paleo sea surface salinities in the low-latitude Atlantic: The δ^{18}O record of *Globigerinoides ruber* (white), Paleoceanography, 10, 749–761, 1995.

Weinkauf, M. F. G., Groeneveld, J., Waniek, J. J., Vennemann, T., and Martini, R.: Stable oxygen isotope composition is biased by shell calcification intensity in planktonic foraminifera, Paleoceanogr. Paleocl., 35, e2020PA003941, https://doi.org/10.1029/2020PA003941, 2020.

Wu, G. and Berger, W. H.: Planktonic foraminifera: differential dissolution and the quaternary stable isotope record in the west equatorial Pacific, Paleoceanography, 4, 181–198, 1989.

Wycech, J. B., Kelly, D. C., Kitajima, K., Kozdon, R., Orland, I. J., and Valley, J. W.: Combined effects of gametogenic calcification and dissolution on δ^{18}O measurements of the planktic foraminifer *Trilobatus sacculifer*, Geochem. Geophys. Geosys., 19, 4487–4501, https://doi.org/10.1029/2018GC007908, 2018.

Zweng, M. M., Reagan, J. R., Seidov, D., Boyer, T. P., Locarnini, R. A., Garcia, H. E., Mishonov, A. V., Baranova, O. K., Weathers, K., Paver, C. R., and Smolyar, I.: World Ocean Atlas 2018, Volume 2: Salinity, edited by: Mishonov, A., NOAA Atlas NESDIS 82, 50 pp., 2018.